Impact of thermal masses on the peak load in district heating systems

Effects of thermal masses on peak formation in district heating system

E. Guelpa

elisa.guelpa@polito.it Politecnico di Torino, Corso Duca degli Abruzzi 24, Torino (Italy)

Abstract

During district heating operations, part of the heat supplied to the network is used for increasing the temperature of the various components (e.g. transport and distribution networks, heat exchangers installed in the substations, heating circuits and heating devices in buildings). The mass of these components acts as thermal storages, storing heat when their temperature increases and releasing heat when they cool down. Their impact may become significant, especially during shutdown or setback. In this paper, the district heating components are analyzed to estimate the impact of their thermal capacity on the thermal demand. This shows a clear image of the thermal supply used to heat the other thermal masses, that can be managed differently since partially independent from the indoor temperature. Results show that in the case study analyzed, i.e. large system mainly switched off during night, the heat absorbed by the thermal masses corresponds to the 4% of the heat supplied during the entire day and 70% of the heat provided during the peak. The various thermal masses affect the extra heat absorbed to a similar extent (except for radiators). Results provide a clue that proper management of thermal masses for energy saving is an interesting option.

Keywords

Thermal capacity district heating, Network storage, Temperature variation, thermal networks, advanced operations

1. Introduction

Through district heating it is possible to produce thermal power for indoor heating purposes in large plants with high performance like combined heat and power (CHP) plants, waste heat from industry or service sectors [1], renewable sources such as geothermal [2], solar [3] etc. However, heat transport and distribution to the various costumers needs a significant infrastructure [4, 5]. This rely on:

a) Supply and return pipelines to supply heat to the costumers and return water to the plants [6].
b) Thermal storages used to store energy produced in case of large availability or low cost [7].
c) Heat exchangers in each building (or group of buildings) to provide heat to the heating circuit [8].
d) The building heating circuit and the heating devices.

All these pieces of infrastructure are subjected to temperature changes during operations. Heat demand significantly varies in a daily perspective. This is quite constant during the daylight hours, lower during the night and higher during the morning. Peaks are usually at their highest at 5-7 am as shown in [9]. Thermal peaks occurs both in the cases of nighttime attenuation and heating systemsswitched off. During peaks, the thermal plants must cover the extra heat needed to increase the indoor building temperature (that are usually lower during night) [10]. During this phase, a part of the heat is used to increase the temperature of the entire infrastructure.

There are various techniques to cover peaks:

- Increasing the heat production in CHP plants. This creates a new constraints for the electricity production that is related to the heat production. This might affect the system competitiveness on the electricity market.
- Use Heat Only Boilers. The main drawback is the low second law performance.
- Thermal storages [11, 12]. These can be small buffers installed in the building or large centralized storages.
- Demand side management (DSM). This consists in managing the building thermal capacities to provide heat when this is more convenient. The heating schedule of buildings or their settings are modified in order to obtain the best profile as possible, from a production perspective [13-15].

In the literature, analyses of district heating network considered as a storage are proposed in [16, 17], to quantify the potential of storing energy in the pipelines beyond that in heat buffers. Also the thermal mass of buildings is analyzed in various paper, specifically to estimate the potential for demand side management [18-20].

In [21], an optimizer is proposed for the district heating management taking into account inertia of both networks and buildings. A rough estimation of the potential of thermal storage capacity of the network is done in [22]; assuming a temperature gap of 10 °C, the thermal storage capacity of the entire Denmark is about 2600 GWh. This is about 10% of the entire Danish thermal storage capacity [23].
However in the literature the contribution of the various thermal masses is usually not considered, neither on the peak formation. Knowledge of the amount of thermal masses of the entire system could be an extremely interesting, to increasing the awareness of its thermal dynamics and the number of components to be exploited as thermal masses during operations. This research path requires preliminary analysis and deep knowledge of design and operational contributions of the network.
This paper represent a detailed analysis of the various thermal masses of the district heating components. The various pieces of infrastructure located between the heat production (thermal plant) and the heat use (building environment) are taken into account. The analysis is performed considering an existing district heating system that is representative of large-size European networks. The various components are studied considering separate simulation or data analysis of substations. The innovative aspect of this work is represented by a quantitative evaluation of the impacts of temperature changes in district heating components during operation. This is useful for an aware management of the networks and for operation improvement.
The paper is structured as follows:

- Section 2 reports the major heat capacities in district heating systems.
- Section 3 reports the case study used for the analysis of the thermal capacities (i.e. an existing network that can be taken as a typical example of a European large district heating network, for both dimension and energy density).
- Section 4 shows the results of a separate analysis of the various components.
- Section 5 reports the comparison of the results from energy and thermal power evolution perspectives.

2. Different types of heat capacities

In district heating systems, various masses (depicted in Fig. 1) change their temperature during operations.

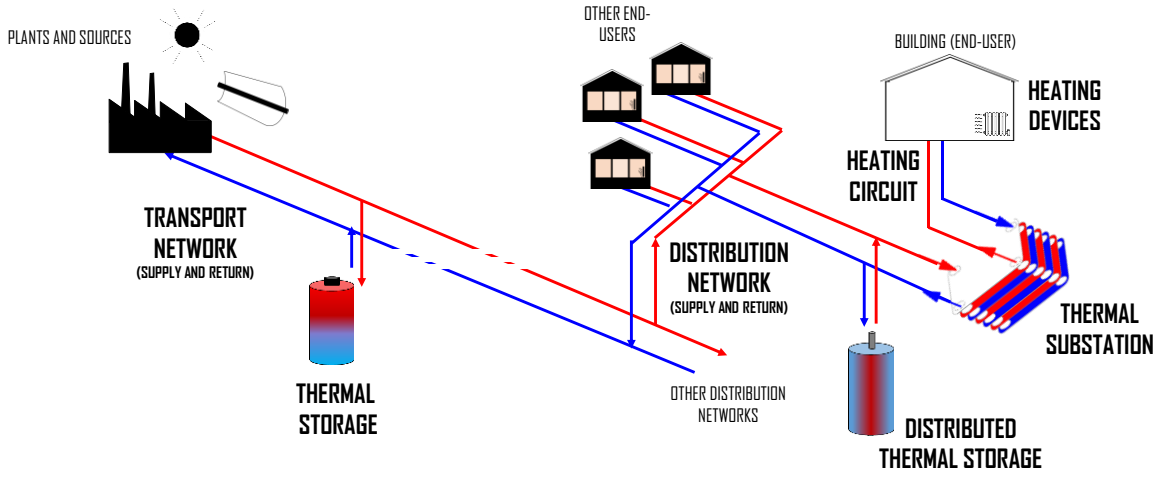

Fig.1 Main thermal masses in district heating systems

The main ones are:

1. *The supply transport network*. This represents the main backbone of the district heating network, consisting of the largest pipelines that transport hot water from the thermal plants to the various urban areas. Water in the supply transport network changes its temperature as a consequence of the control strategy (when the heat demand is adjusted by temperature variation) and during night shutdown or setback, when the mass flow rates can be very small and the impact of losses quite large.
2. *The supply distribution networks*. These are the small networks connecting the transport network to the costumers (as shown in Fig 1). The distribution networks are characterized by small pipelines (usually with diameters smaller than 0.2 m), that when the thermal demand is zero, significantly reduce their temperature because of high impact of thermal losses.

3. *The thermal storages* (mainly water sensible storage) are usually installed as buffer in district heating network and significantly change their temperature during their operations.
4. *The heat exchangers installed in the substations* which connect the building heating systems with the distribution network. In case of night shutdown, this device reaches a temperature which can be close to the temperature of the technical room.
5. *The heating circuit of the building.* This includes the pipes connecting the substation heat exchanger to the various heating devices (radiators, radiant floors etc.). The water inside the pipelines during the shutdowns reaches low temperature, usually the indoor temperature.
6. *The heating devices.* These are mainly radiators and radiant floors that before reaching the steady state operations needs heat to increase their own temperature.
7. *Possible distributed thermal storages* installed in the substations. These must have small volume in order to be installed in the technical room where the substation is also located. For this aim, latent heat storages represent an interesting option [24, 25].
8. *The building thermal mass.* This includes the building envelope of the that may play a major role in case of old or significantly insulated buildings.
9. *The return distribution networks.* These are the small networks connecting the costumer substations to the transport return network. These pipelines during the night shutdown reach low temperature, closer to the environmental temperature than to the supply temperature. The return temperature level can change a lot since in case of low thermal demand the heat exchanger efficacy increases (and the return temperature decreases).
10. *The return transport network*, connects the return distribution networks to the thermal plants. This is also subject to temperature variations as a consequence of the supply temperature variation, the thermal power absorbed by the costumers, the thermal losses and the heat absorbed by the masses installed upstream.

The cited masses are connected as shown in Fig. 2, therefore it is not possible to charge the downstream systems (increasing their temperature), without charging (at least partially) the upstream systems. For instance, it is not possible increase temperature of the substation heat exchanger if the temperature of the supply network is low. This makes the management of the system quite complicated and strongly dependent on the network topology and the dimension/type of the components.

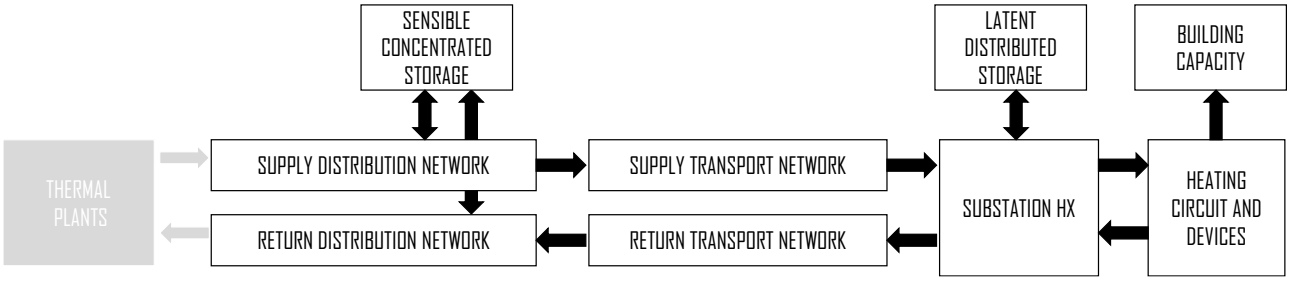

Fig.2 Cascade fluxes of the thermal masses in district heating systems

3. Case Study

The system analyzed in this paper is the Turin district heating network. This is composed of a transport network connecting the thermal plants to the distribution networks (large diameter pipelines) and various distribution networks connecting the transport network to about 8000 buildings. In the Turin network, there are 5 production sites (including 2 cogeneration plants, 4 heat only boilers and 12 concentrated storage). Fig. 3 depicts the transport network with the production sites and three out of 182 distribution networks.

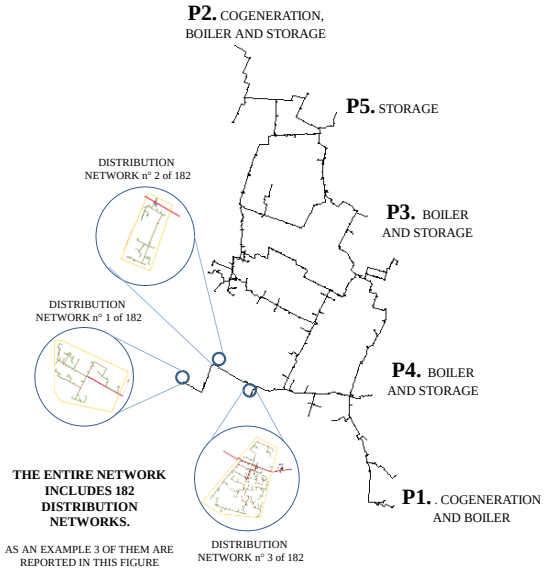

Fig. 3. Schematic of Turin District Heating Network: the transport pipeline and in evidence the thermal plants and three distribution networks.

The water supply temperature is constant at about 120°C. The Turin District heating is the largest in Italy and among the largest in Europe (56 million m3 of buildings connected, 800 K inhabitants and 800 km of pipelines). Additional data on the daily and annual demand are reported in Tab. 1.

Annual demand	2	TWh
Maximum peak	1.3	GW
Daily Demand	8 - 15	GWh

Table 1. Details for the Turin district heating thermal demand

The Turin district heating network can be considered as a case study representative of a typical large European network, for three main reason: a) the large (but not extremely large as the Moscow network) dimension as can be noticed by the Fig. 4 [26] b)the thermal demand for unit of area is around 750 MJ/m^2 that is near to the average of the urban demand of cities served by district heating in other European countries [27] c) this is a second generation network, as various European large scale networks.

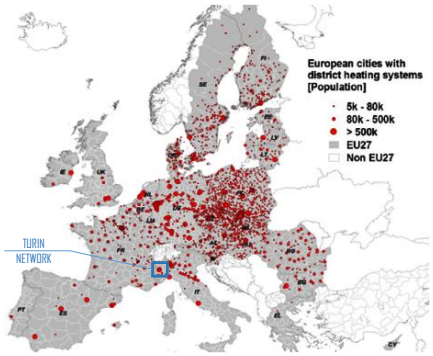

Fig. 4. European District Heating Networks [26]: the Turin system as an example of a large size DH.

For the present analysis the daily operations are considered. During the final part of the morning and the afternoon, the thermal demand is subject to small variations since the indoor temperature is at the set point value. During night, the thermal demand usually decreases. This is due to two main reasons: a) the habit of the occupants b) the possibility of reducing the energy consumption. During night, two types of control can be

adopted: 1) the heating system of the users are completely shut-down; 2) the regulation set point changes during the night such that a minor amount of heat is provided to the buildings. The first approach is particularly used in the Mediterranean areas. The second one is more used in the North Europe areas. In both the cases there are some buildings requiring heat during the entire 24 hours, such as hospitals.

In this paper, the case of night shutdown is considered in order to quantify the impact of the thermal capacities in the peak formation.

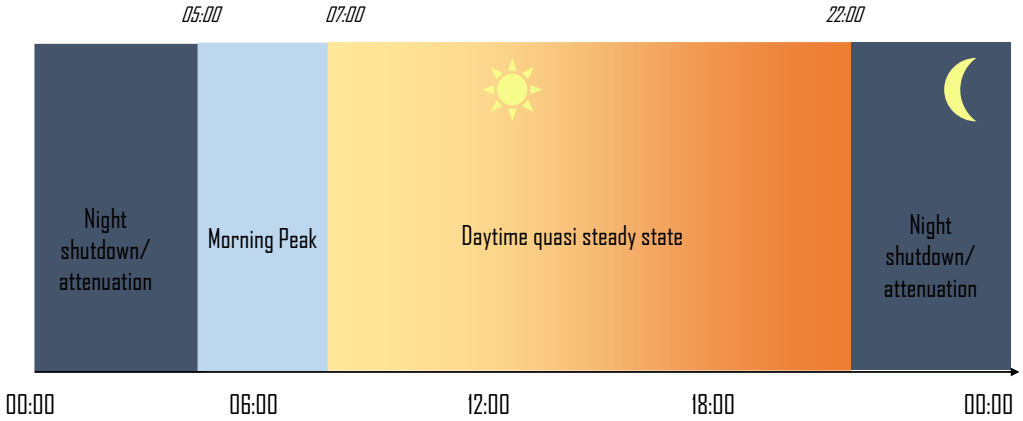

Fig. 5. Daily operations in district heating

4. Methodology and evaluation results

In general the equation for the evaluation of thermal power absorbed/released by the thermal masses (Φ_{abs}) and the related energy absorbed/released in a period (E_{abs}) are:

$$\phi_{abs} = m\frac{\partial H}{\partial t} = mc\frac{\partial T}{\partial t} + m\frac{\partial L}{\partial t} \quad (1)$$

$$E_{abs} = \int_{t1}^{t2} \phi_{abs}\, dt \quad (2)$$

where m is the mass, c the specific heat, t the time, H is the total enthalpy, i.e. the sum of the sensible and the latent contribution *L*. In some cases, the evaluation of the heat absorbed evolution is not straightforward since it changes in time. In the following subsections the way for evaluating the energy and the thermal power and the preliminary results are shown individually for the various thermal masses. The building thermal mass is not considered since this have still been analyzed in several papers *ad hoc* in the literature, and results are reported [18-20, 29]. As shown in the result section the contribution of the building is significant although this is not the only responsible for the peak formation.

4.1 Network pipelines

In the case of the thermal power absorbed/released by the pipeline Eq. 1 can be rewritten for each pipe of the system considering the specific heat and the density constant in the considered temperature range as follows:

$$\phi_{abs\_NET} = mc\frac{\partial T(t,x,y)}{\partial t} = c\rho \sum_{i=1}^{n\_p} L_i \frac{\pi D_i^2}{4}\frac{\partial T(t,A,G)}{\partial t} \quad (3)$$

where m is the mass, c the specific heat, t the time, ρ the water density, T the temperature x and y are the spatial coordinates of the district heating system, A is incidence matrix that represents the network topology, G is the vector of mass flow rates located in the system D and L respectively the diameters and the length of the pipelines.
The thermal mass in the transport network is large because the mass of water is large. Temperature variations during the operations are usually small, not above 10°C. These are due to two main reasons: 1) the water temperature can be increased for control purposes to provide more (or less) heat to the users (although the regulation is usually done mainly on mass flow rates) and 2) during the night the thermal request are small (and thus the mass flow rates) so the thermal losses have larger impact. Thermal losses may create temperature gradients of the order of some degrees especially when mass flow rates are lower than 10-20% of the nominal values. If we consider the network pipelines as a storage, during the night the system is discharged. That means that the temperature must be restored during the early morning. Charging the pipelines is necessary for system operation.
As indicated in Eq. 3 evaluation of the heat stored in the pipeline relies on the knowledge of the temperature field in the district heating network. The temperature field in the pipelines can be evaluated using a network thermo-fluidynamic model. The model solves mass, momentum and energy conservation equations in all the pipelines of the network. The network topology is taken into account through the incidence matrix $\boldsymbol{A}$, which allows expressing the interconnection between the pipelines. This is done considering the district heating network as a graph, i.e. a system of nodes and branches. Mass and momentum conservation problems can be considered in steady state since the pressure variations travel at a velocity much faster than the fluid velocity. The mass conservation equation consists in a mass balance of the mass flow entering and exiting each node. The momentum equation includes the terms related to the friction losses and the pumping power provided by the booster pumping stations. The momentum conservation equation provides a relation between pressures and mass flow rates in the network. Since the relation is non-linear, mass and momentum conservation equations are solved by means of an iterative approach. As concerning the energy conservation equation this is unsteady since the temperature variations travel with the water velocity; clearly this includes the thermal losses towards the environment. The mass, momentum and energy conservation equation written in a matrix form are reported in Eq. (4-6)

$$\mathbf{A} \cdot \mathbf{G} + \mathbf{G}_{\mathrm{BC}} = 0 \tag{4}$$

$$\mathbf{G} = \mathbf{R}^{-1} \cdot \mathbf{A}^{\mathrm{T}} \cdot \mathbf{P} + \mathbf{R}^{-1} \cdot \Delta \mathbf{P}_{\boldsymbol{P}} \tag{5}$$

$$\mathbf{M}\dot{\mathbf{T}} + \mathbf{K}\mathbf{T} = \mathbf{f} \tag{6}$$

where G, P and T are the unknown (i.e. respectively the mass flow, the pressure and the temperature matrices), M and K the mass and stiffness matrix (typical of advection problems), A the incidence matrix, R the fluidynamic resistance, G_{BC} the mass flow boundary conditions and ΔP_P the pressure gap due to pumping systems. The thermo-fluidynamic model is used to estimate the evolution of the temperature in time within the network. The same approach can be used for the transport networks and the distribution networks. Details about the simulation mode adopted for the analysis are reported in Table 2.

Model adopted	thermo-fluidynamic model developed, tested and validated at Politecnico di Torino [30]
Boundary conditions for supply network	mass flows and temperature at the inlet node (mass flow from the thermal plants)
Boundary conditions for return network	mass flows and temperature at the inlet node (mass flow from the buildings)
Initial condition	evaluated by preliminary analysis simulating the previous transient.

Table 2. Details for the adopted simulation model

Fig. 6 shows the results obtained for the supply transport network. The distribution of water temperature along the pipelines is reported for two different time frames. The first time frame considered, is just before the costumer systems are switched on in the morning at 5 AM. The second is after the morning peak, at 8 AM. In the first case it is possible to notice that the temperature values are lower in the central area of the network because the two cogeneration plants, that are located respectively at the northernmost and southernmost part of the network, supply the heat required at night (map on the left). Because of the thermal losses due to the low mass flow rate circulating, the temperatures decrease with respect a daylight period and the network "discharges". Later in the morning, at 8 AM, because of the larger mass flow rates supplied to the buildings during the two previous hours the temperature of water in the pipelines increases (map at the right in the figure). During this transient, the network is "charged" since its temperature increases.

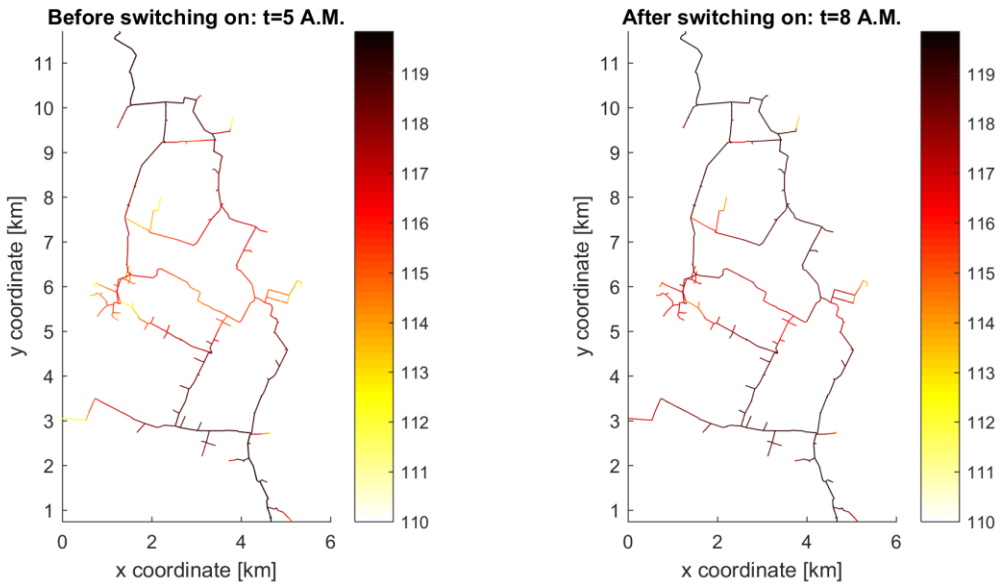

Fig.6 Results: temperature fields (in °C) along a main district heating network (supply pipeline)

Fig. 7 shows the temperature distribution within the network pipelines at different times during the start-up evolution in a distribution network. In this case, the return line is shown. Temperatures during the night transient reach about 35-40 °C. During the start up the network is charged and the temperature increases. Clearly, the temperature pattern depends from the scheduling of the customer requests. However time after time the network increases its temperature and this is charged in about 1-3 hours depending in the difference between the costumer schedules.

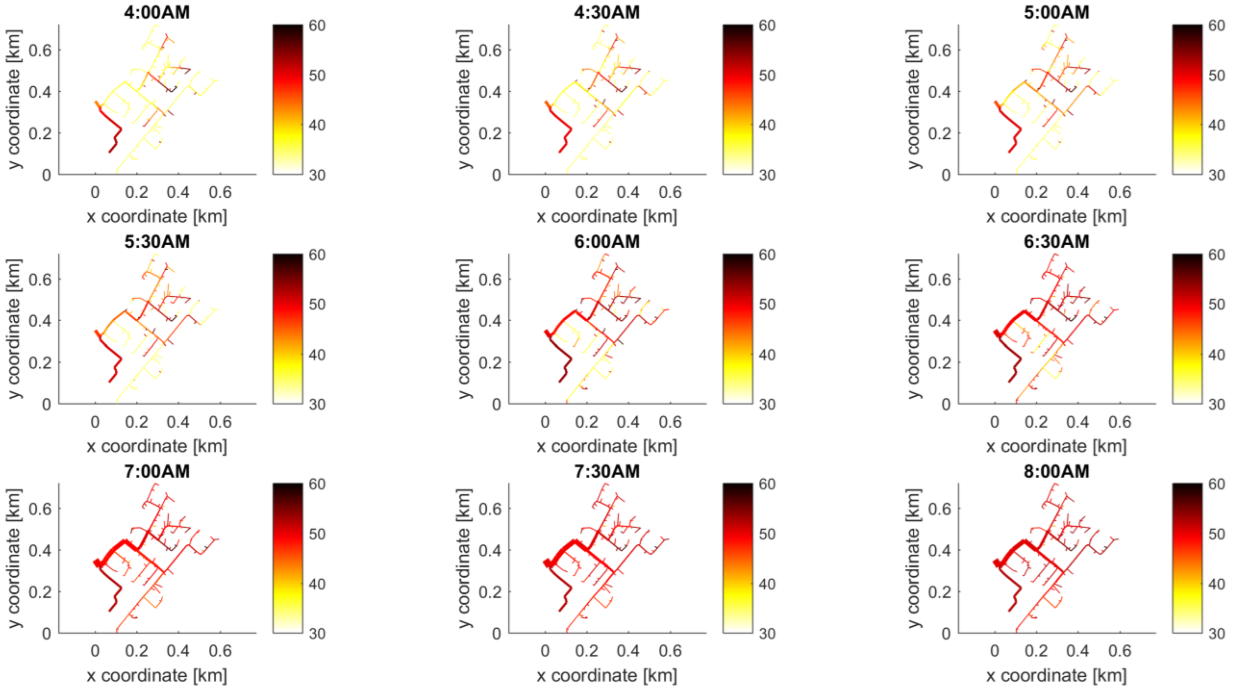

Fig.7 Results: temperature fields (in °C) along a distribution network (return pipeline)

4.2 Substation Heat exchangers

Calculation of the energy absorbed during start-up by all the devices installed in a substation it is not straightforward. The plates of the heat exchangers represent one of the mass that are heated during the morning. Some example of other masses are the external envelope of the heat exchanger, the technical components for mechanical holding the junctions and the various devices installed. Also fouling has a non-negligible contribution [25]. The evaluation of the heat absorbed by the heat exchanger is done by using the data measured at the substation for billing purposes. A schematic of a substation in shown in Fig. 8. Temperature T1, T2, T3 and T4 and mass flow rate at the primary side $\dot{m}_h$ are usually collected during operations.

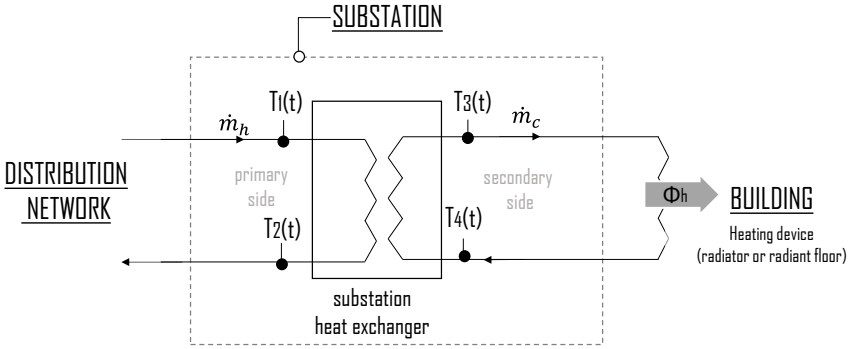

Fig. 8 Substation schematic

The data stored each 5 minutes can be used to evaluate:

- the thermal power provided to the heat exchanger by the supply line (Eq. 7).

$$\phi_{\text{prim\_side}} = \dot{m}_h \, c_p (T_1 - T_2) \tag{7}$$

- The thermal power provided to the secondary circuit (Eq. 8).

$$\phi_{\text{sec\_side}} = \dot{m}_c \, c_p (T_3 - T_4) \tag{8}$$

The difference between the heat supplied to the heat exchanger and the heat absorbed by the fluid in the secondary circuit provides a measure of the heat that is absorbed by the substation components (Eq. 9). Thermal losses can be neglected since plate heat exchanger installed in the thermal substation are compact and usually highly insulated such that losses are minor.

$$\sum_{i=1}^{n\_comp} m_i \, c_i \, \frac{dT_i}{dt} = \phi_{\text{prim\_side}} - \phi_{\text{sec\_side}} \tag{9}$$

Actually, the mass flow rate in the secondary circuit $\dot{m}_c$ is not known. This is constant in most of the buildings since variable speed pumps are usually not installed in the heating circuits. The mass flow rate $\dot{m}_c$ has been estimated by mean of a preliminary analysis of the data. The following procedure has been used:

1. The afternoon thermal transient is evaluated by mean of a routine, that allows finding a time frame during the day with a quasi-steady state thermal demand.
2. Since in case of steady-state conditions the heat provided to the heat exchanger is equal to the heat provided to the secondary circuit the mass flow rate can be estimated by using Eq. 10.

$$0 = \phi_{\text{prim\_side}} - \phi_{\text{sec\_side}} = \dot{m}_h \, c_p (T_1 - T_2) - \dot{m}_c \, c_p (T_3 - T_4) \tag{10}$$

The evolution of ϕ_{prim_side} and ϕ_{sec_side} evaluated for 6 different substations are reported in Fig. 9 respectively in black and red. The evolution are not perfectly overlapped in the steady state conditions mainly because of the small errors in data detection and because of the estimation of $\dot{m}_c$ by means of an analysis of the rough data. If in the steady state conditions the two heat fluxes fluctuate around the same mean value, during the start-up (when the thermal peak occur) they differ significantly. This difference is due to the contribution of the heat absorbed by the substation devices to increase their temperature during the start-up. This can be used to estimate the thermal mass of the substation device. This is done by supposing that all the components vary their temperature from the temperature of 15°C (a typical temperature of the technical room) and the mean temperature of the heat exchanger in steady state conditions of 75 °C.

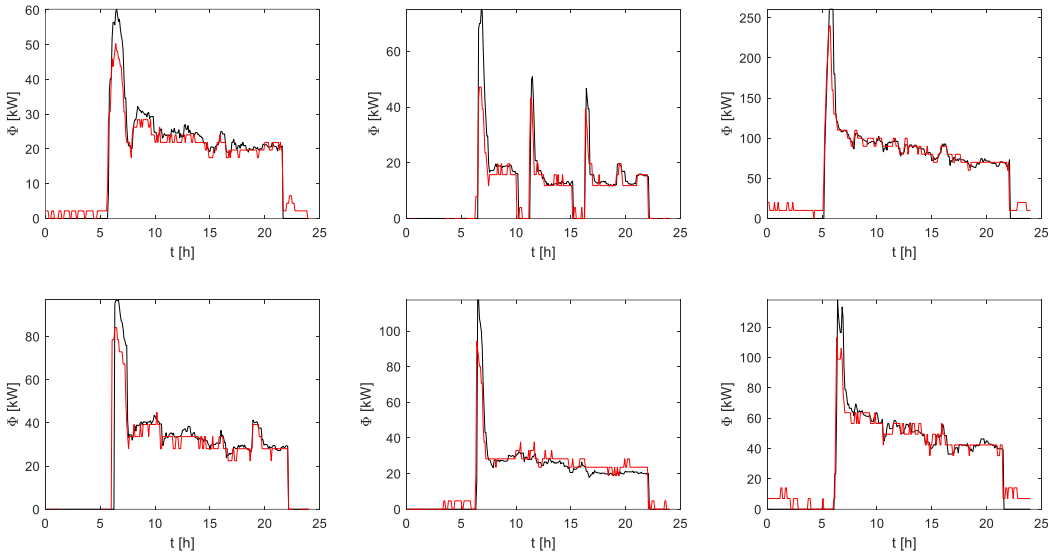

Fig. 9 Comparison of the heat flux absorbed (black) and emitted (red) by the heat exchanger. The difference during the start up is used to determine the heat exchanger thermal capacity

The heat capacity obtained by the analysis of the peak transient for various medium size heat exchangers is around 10 kWh. By taking into account only the heat absorbed by the plates of the heat exchanger of stainless steel for a medium size costumer the value achieved is about one third of 10 kWh. This means that the extra amount of heat is absorbed by the supplementary material in the substations (water, pipes, etc).

4.3 Heating circuit

Considering the heating circuit, the estimation of the energy absorbed can be obtained as follows:

$$E_{abs\_HC} = \int m_w c_w \frac{dT}{dt}\, dt = m_w c_w \Delta T \tag{11}$$

It is possible to suppose that:

- in case of radiators the quantity of water needed is about 6 l/kW installed [31, 32];
- during the night the entire mass cool down to the indoor temperature (about 20°C);
- during the morning the entire mass is heated to the design temperature (60°C-70°C in the case of radiator);
- some of the entire amount of buildings connected to the system do not switch off the heating system during the night, since special buildings (like hospitals) require heat during all the 24 h.

4.4 Heating devices

When the supply line of the secondary circuit is heated, the heating devices are crossed over by the hot heat transfer fluid. A first portion of heat released by the heat transfer fluid is mainly absorbed by the heating device mass, which increases its temperature. The equation describing the heat exchange within the heating device is:

$$\phi_{abs\_HD} = m \frac{\partial H}{\partial t} = mc \frac{\partial T}{\partial t} \tag{12}$$

The heat that can be absorbed depends on the type of heating device. These are mainly radiator and radiant floors. Equations for the evaluation of heat absorbed are Eq. 13 and 14.

$$q_{abs\_RAD} = \int_{t_{su}}^{t_{ss}} mc \frac{dT}{dt}\, dt = mc(T_{in} - T_{av_{fin}}) \quad (13)$$

$$q_{abs\_RADFLOOR} = \iiint_{t_{su}}^{t_{ss}} mc \frac{\partial T(t,x,y)}{\partial t}\, dt\, dy\, dx \quad (14)$$

In case of radiators, the evaluation of the capacity is simpler since the entire system can be considered as a concentrated mass reaching the same final average temperature, equal to the mean water temperature (Eq. 13). Radiant floor is a very interesting application for exploiting building capacity since floor and subfloor have relevant masses with respect to the radiators. In case of radiant floor, the evaluation is more complicated since the water pipes are sealed in the subfloor, as shown in Eq. 5. In this case, the entire mass of the subfloor does not reach the same temperature. For this reason, the evaluation of the energy storable in subfloor should rely in experiment or simulation. For the aim of this work a numerical simulation is used. The computational domain considered and the mesh used is reported in Fig. 10. A finite element scheme has been applied to the domain and solved by using the software COMSOL®. Details on the simulation are reported in Tab. 3.

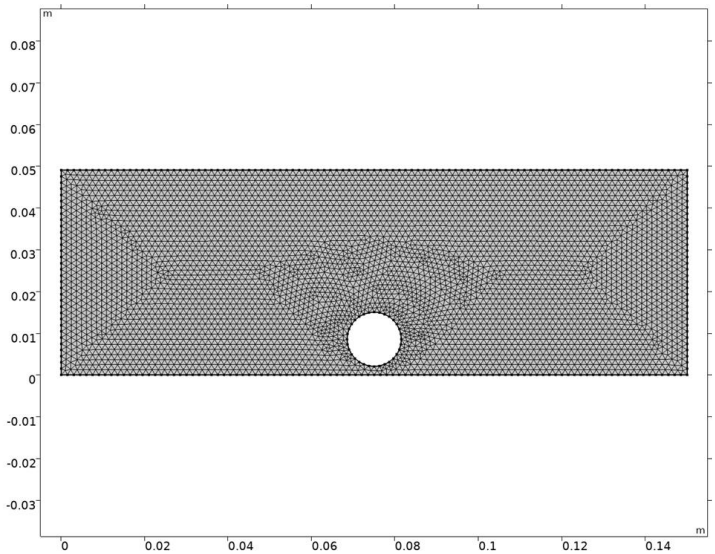

Fig.10 Computational domain of a radiant floor

number of mesh	8782 elements
buondary conditions	20 °C for the upper boundary (indoor temperature) and 40 °C for the pipe boundary and adiabaticity for the other boundaries
initial condition	evaluated by preliminary analysis simulating the previous transient.
thermal conductivity	1 W/m K
convergence criteria	1 E-6

Tab. 3 Details on the radiant floor simulation model

The heat that can be absorbed by the subfloor is estimated by considering the limitation of maximum temperature for the floor surface (29 °C). For this reason, the temperature of water flowing the pipelines are selected accordingly. Fig. 11 shows two results of the subfloor simulation in steady state conditions. The temperature distribution is shown. In the surrounding of the pipe the temperature is similar to the temperature of the water flowing the pipe, while in part of the subfloor this is at lower temperature, more similar to the surface temperature. For this reason, approximate the subfloor temperature with the water temperature should create significant difference in the results achieved. Temperature ranges between 40°C to 25 °C. In both the cases, the temperature at the top complies with the constraint of 29°C.

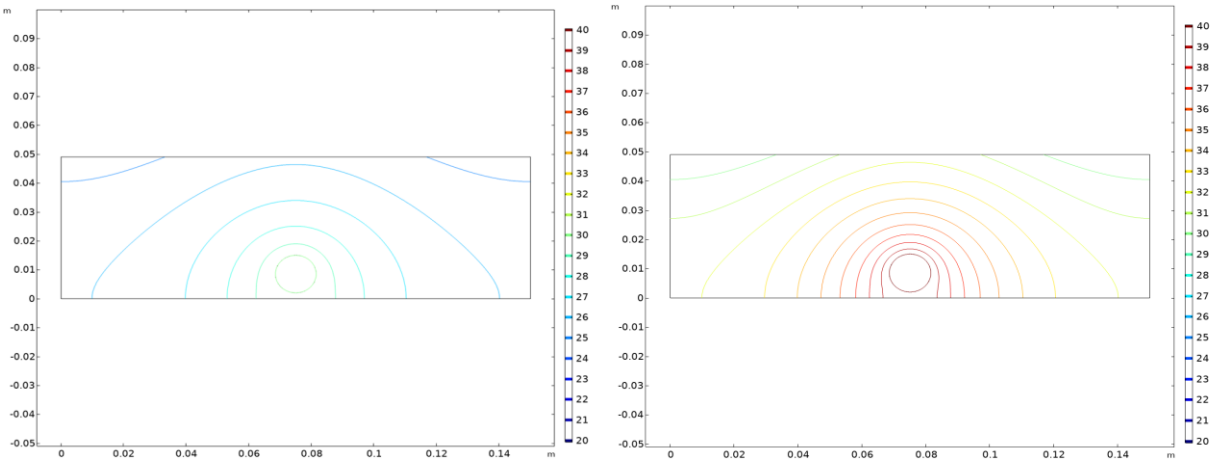

(a) (b)

Fig. 11 Simulation results. Temperarture field in the subfloor for floor heating a) Twater=30°C b) Twater=40°C

4.5 Additional thermal capacities (Thermal Storages)

Concerning the thermal storages, the energy storable in a district heating system mainly depends on:

1. The space availability for the storage. In urban areas, cost of land is not negligible and space availability suitable for the storing purpose is usually constrained.
2. The temperature of the heat supplied to the district heating (corresponding to the district heating generation) and more specifically on the temperature gap between supply and return. In case of low temperature difference, a lower amount of energy can be stored in the same volume.

The energy can be stored using concentrated or distributed thermal storage. In the first case, a low number of large water tanks are installed in strategic areas of the city. In the second case a number of small thermal storages are installed in the building substation, operating in combination with the substation heat exchanger.
Concerning concentrated thermal storage, an analysis is performed in order to evaluate the amount of energy that can be stored by varying the district heating generation and the number of storages installed.
Fig. 12 depicts the energy stored in a district heating system as a function of the number of thermal storages and on the district heating generations (that differs on supply and return temperature as shown in [33]). The storage size considered is 500 m^3 that is an average size for district heating installation in urban areas. The energy that can be stored varies from 50 to 600 MWh. Obviously the higher the number of storages, the larger the amount of energy storable. The crucial information provided by Fig. 12 is the dramatic decrease of the energy storable in sensible water storage while moving towards new district heating generations. This means that in the existing networks the available thermal storages will decrease their storing potential, while reducing the supply temperature. In the same way, the number of storages necessary to reach a certain storage capacity is much higher in case of 4th generation networks. The figure shows that in case of large district heating with 15 storage installed the energy storable is less than a third in case of 4th generation systems respect to the 2nd generation systems.

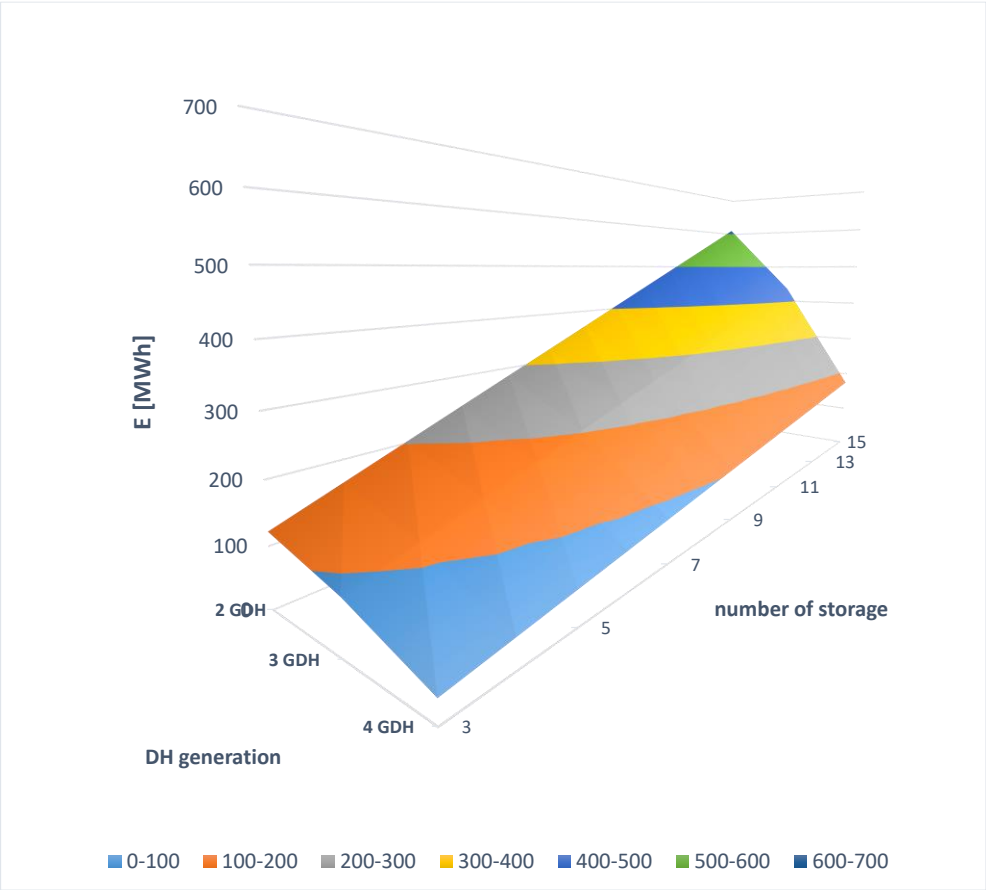

Fig. 12 Energy storable by means of concentrated thermal storage in district heating systems

In case of distributed heat storage (in the building substations), the installation of latent heat storages (filled with Phase Change Materials (PCM)) is preferred, at least in a future perspective. In this case, the thermal power stored and released varies in time. This is mainly due to the variation of the thermal conductivity of the PCM the storage is filled and the temperature variation of the PCM.
For this reason, it makes sense to evaluate the heat flux evolution. This can be done by mean of a 2D thermo-fluidynamic model of the system. The thermo-fluidynamic model allows to takes into account the effect of the phase variation occurring in the thermal storage and the effect of the buoyancy. The domain is schematized in Fig. 13. For this study a small portion of matter is considered, including both PCM (paraffin wax) and water (radially 0.04 m PCM and 0.015 m water). The contribution of the conduction in the pipeline (steel) is considered only as a discontinuity because of its negligible contribution. Mesh dimension is 1 mm, except for the use of a boundary layer to refine solution at the interfaces. The selected mesh dimension has been proved to be sufficiently fine to not affect the results. Velocity and temperature boundary conditions are imposed at the inlet water section, and adiabaticity at the boundaries of the PCM. An inlet temperature condition is used.

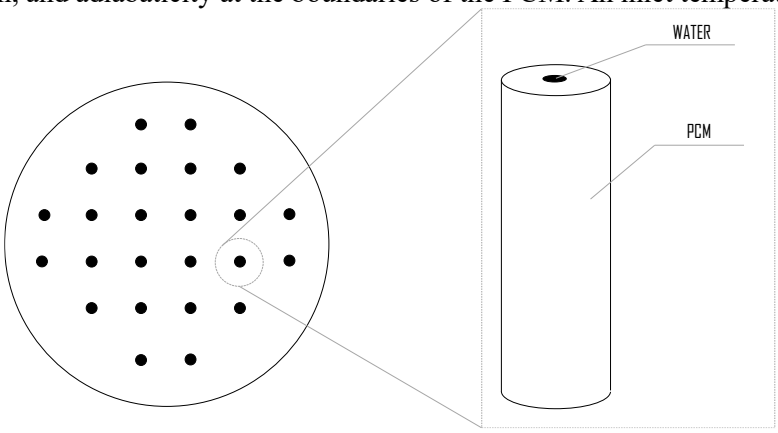

Fig. 13 Energy storable by means of concentrated thermal storage in district heating systems

An axial-symmetric unsteady problem 2D is solved by an implicit discretization with a control volume approach. The software Fluent has been adopted. Second order discretization in time is used. The water stream is laminar. Solidifation/melting is simulated with a mushy zone approach (porosity approach). The equation solved is:

$$\frac{\partial}{\partial t}(\rho H) + \nabla \cdot (\rho \vec{v} H) = \nabla \cdot (k \nabla T) + S \quad (15)$$

Where the enthalpy is defined as:

$$H = h_{ref} + \int_{T_{ref}}^{T} c_p \, dT + \beta L \quad (16)$$

β is equal to 0 in case of solid 1 in case of liquid and a fraction in case of temperature included in the phase change range. The natural convection is modeled by the Boussinesq model, because of the low temperature gradient. Details on the simulation are provided in Tab. 4.

mesh dimension	0.001 m
boundary conditions	WATER: inlet fluid velocity and temperature PCM: Adiabaticity at the boundaries except for the pipe boundary.
initial conditions	completely charged (T= 80°C)
convergences residual (energy)	1 E-6
convergences residual (continuity and momentum)	1 E -3

Tab. 4 Details on the latent heat storage simulation model

This allows estimating the heat evolution of heat in time for a thermal storage installed in a DH substation. Results are reported in Fig. 14. The heat flux normalized is reported for two different sections of the system, one at the top and one at the bottom. The two evolutions are different because of the different temperature of the water flowing in the system at the two different sections and because of the buoyancy effect. In both the sections, the heat flux is maximum in the initial part of the discharge. Than this decreases differently, following the evolution reported in Fig. 14 depending on the cross section considered.

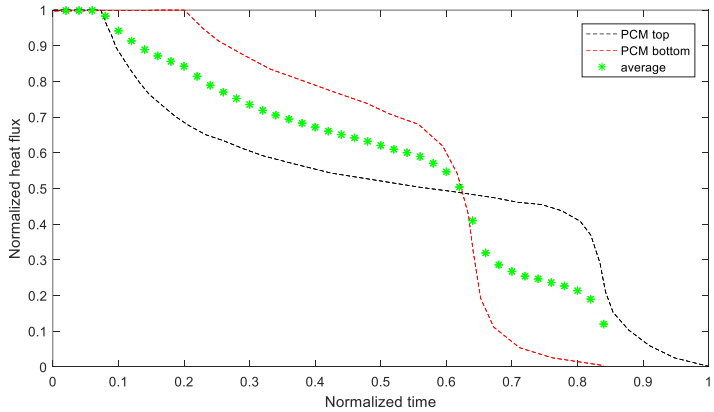

Fig.14 Energy released by a latent heat storage for district heating purposes

5. Comparison

The analysis of the energy absorbed/released by the various masses during the start-up transient of a district heating network allows the evaluation of the heat absorbed during the daily operations. A comparison of the heat absorbed/released is reported in Fig. 15. In the figure are compared:

- The heat absorbed by the transport network.
- The heat absorbed by the distribution networks in order to reach the daily operation temperature, starting from the night asymptotic temperature.
- The heat absorbed by the devices installed in the building substations.
- The heat absorbed by the heating circuits of the buildings.
- The heat absorbed by the radiators.
- The heat that should be absorbed by the subfloor by the radiant floor in order to reach the steady state condition.

In order to provide a clear idea of the amount of energy that is supplied to these components to be charged, a red line is reported. This corresponds to:

- The heat that can be stored in 1 large size water thermal storage of 1000 m^3 (or equivalently two medium size 500 m^3), with a temperature difference of 50 K.
- As an alternative, the heat that could be released if one out of eight buildings of the district heating system is equipped with a latent heat storage of a net PCM volume of 1 m^3 (with a temperature difference of 50 K and the latent enthalpy 160 kJ/kg).

The main piece of information provided by the results reported in Fig. 15 is the large amount of heat that is stored within the various components. All the components, except for the radiators, store an amount of heat larger than the storable in 1000 m^3 of water. This is a significant result since clearly indicates that the influence of thermal capacities shouldn't be ignored during the DH transient analysis.
Furthermore from Fig. 15 it is possible to notice that the building heating circuits and the distribution networks are the two main thermal masses. This is because of the large heat capacity of the water and because in these systems the mass flow rate is completely stopped during night and temperature drops significantly. The radiators represent instead the less significant thermal mass in district heating.

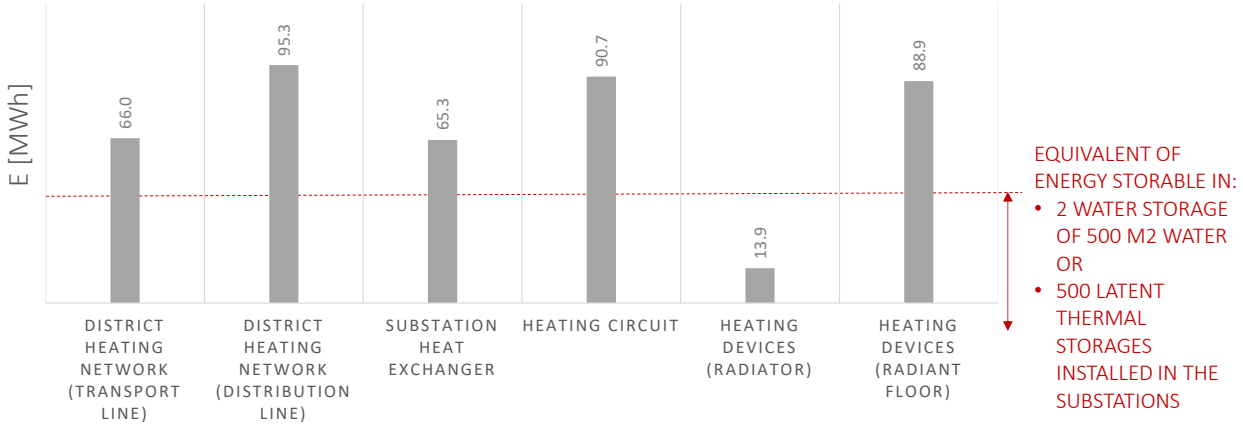

Fig.15 Comparison of the energy absorbed/released by the various part of a district heating system during the start-up transient

Fig. 16 shows the evolution of the thermal power absorbed and released by the various parts of a district heating due to their temperature change. In this specific case, the Turin DH system is analyzed: the concentrated storage available in the real system (12.500 m^3) and radiators, which are the heating devices mainly used up to now are considered. Furthermore, the option of distributed storages installed in one tenth of the substations (with a volume 1.5 m^3) is taken into account, since it could be an option to shave the morning peak. This is a large amount of thermal storage (about 500 units). The positive sign of the curves in Fig. 16 means that the system is discharged (heat exiting), while the negative sign means that the system is charged (heat entering). The two thermal storages behave oppositely to the other thermal masses. These are charged when the thermal masses are discharged (in the evening/night) and they are discharged in the morning during the charging of the thermal masses. For the analysis it has been supposed that all the systems are switched on and off at the same time.
Fig. 16 shows that the amount of heat that can be stored in the sensible thermal storages (black dashed line) is significantly larger than the heat to be supplied to the various thermal masses. As concern the latent heat storage,

the energy released in the morning is larger than the energy required by the other components but these are of the same order of magnitude. The two storages behave differently since the latent heat storage have a variable heat release rate.
An important outcome that can be observed is that, despite the heat released by the thermal storages during the morning is much higher than the heat that must be provided to the various components, when the summation of the heat absorbed by the various thermal masses is considered, things are different. In fact, the sum of the heat absorbed by the entire network, the thermal substations, the heating circuits and the heating devices (0.33 GWh) and the heat released by the sensible thermal storage (0.44 GWh) are similar. This means that the amount of thermal energy stored in the concentrated thermal storages a significant part of the heat used in order to heat the various masses in the system. This result is extremely significant. This suggests that the thermal capacity may have a strongly impact in the district heating operations and that smart regulation strategies should be properly implemented to feed efficiently the network.
The thermal request reported in Fig. 16 is evaluated neglecting the effects of the communication among the thermal masses. Following this approach the values of the thermal request are independent of the others and it is possible to sum the various contributions to obtain the overall thermal demand. It should be interesting to analyze the *cascade effect* that occurs when a thermal mass charges. During the charging transient of a mass the following can be subjected to a discharging effects. The *cascade effect* can be analyzed by mean of a proper model that connects the various components, like various connected storages while charging and discharging phases and being included in optimization tools for district heating management [34, 35]. Optimization tools including thermal capacities effects can provide significant benefits when a proper performance analysis is adopted [36]. This is out of the goals of this work, but it could be useful to properly analyze the impact of a change on the downstream thermal masses.

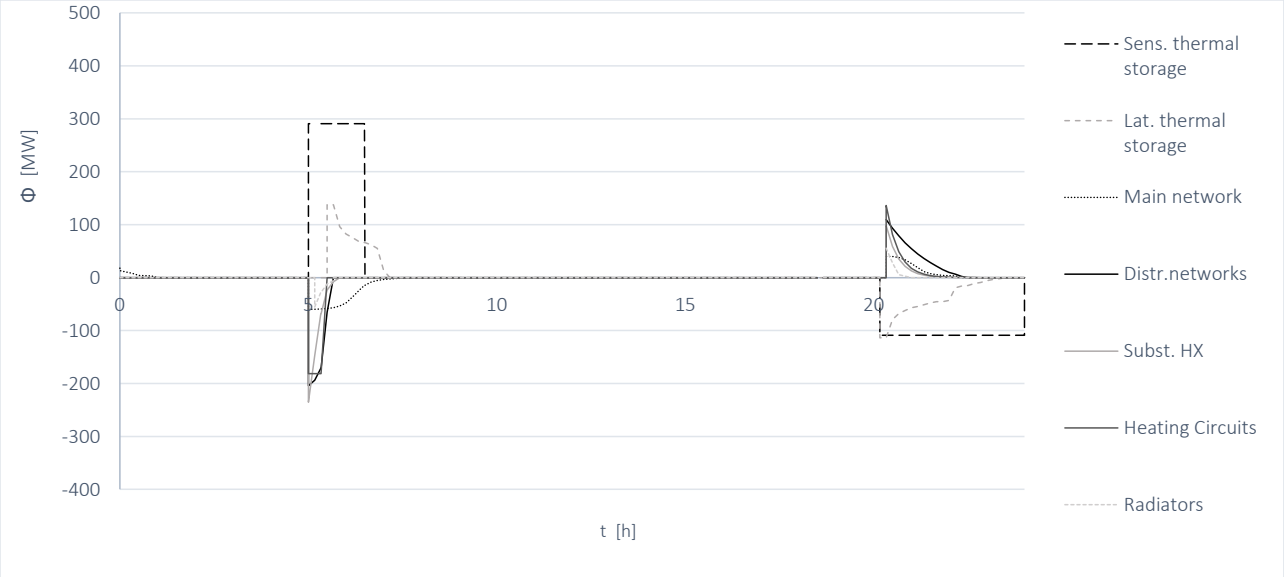

Fig.16 Evolution of thermal power absorbed/released by the various part of a district heating system during a typical daily operation

Fig. 16 clearly shows that a non-negligible amount of heat is required during early morning to heat all these components. It can be interesting to compare total amount of heat required during the morning peak to the heat required to increase the temperature of the thermal mass. This allows also quantifying which is the fraction of heat required to heat the thermal masses and the heat required to increase the indoor temperature. For this reason a supplementary analysis has been conducted in order to quantify the contribution of the thermal masses in the creation of the morning peak; results are shown in Fig. 17 (right). The histogram includes:

- The extra energy absorbed by the network during the morning peak, respect to the quasi steady state operations occurring after 9 AM (shown in Fig. 17, left).
- The energy required for heating the district heating thermal masses. This has been obtained as the summation of the thermal energy required by the transport network, distribution network, substations, heating circuit and radiators.

- The energy used for space heating (the difference between the first and the second bar).

Fig. 17 shows that the extra energy required during the thermal peak (0.4 GWh) is mostly used to heat the system thermal masses (0.33 GWh). This means that the peak occurs mainly to provide heat to the system components while the necessity of increasing the temperature of buildings after the night switching off affects the peak to a lesser extent. In particular the daily fraction of heat required to the various devices to increase their temperature is: 1.2% for the heating circuits, 1.1% for the distribution networks, 0.8% for both the transport network and substation heat exchanger and 0.2% for the radiators.

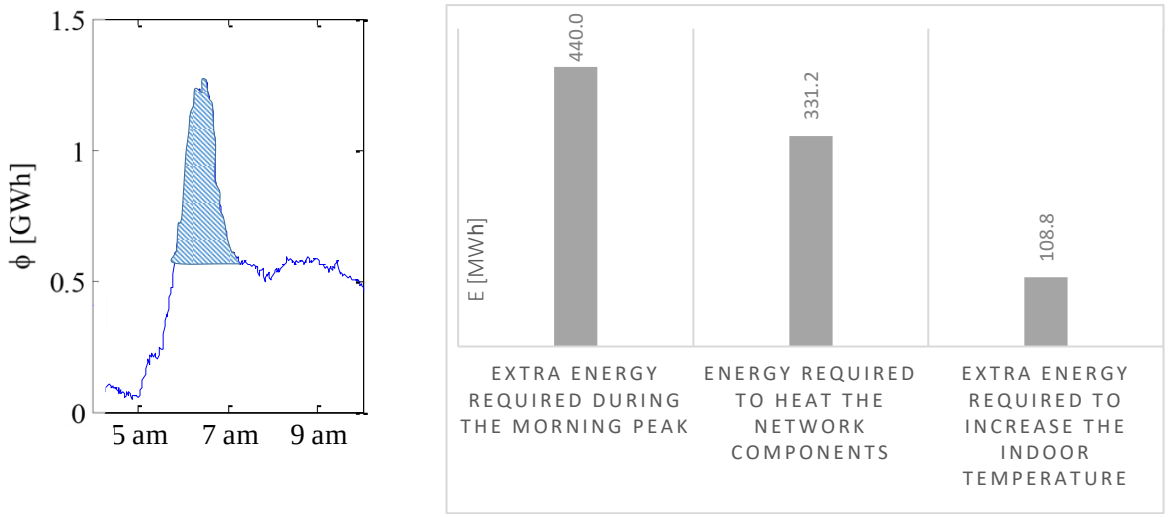

Fig.17 Left: Extra energy required during peak. Right: Composition of the extra energy required during the peak: heat for increasing the thermal mass temperature and heat required for increasing the indoor temperature after the night shutdown. The summation of the second and the third column gives the first one.

6. Conclusion

In this paper, the thermal masses of a district heating network and their impact on the peak demand are analyzed. This is done with the aim of understanding the effects of the network regulation on the thermal request. Network pipelines, thermal storages, thermal substations, heating circuits and heating devices have been considered in the analysis. Numerical simulations along with experimental test results are used to find, for each component, an approach for the evaluation of its behavior during the district heating operations. The approaches proposed have been applied to the Turin network that is representative of a European large size network. Results of the analysis show that none of the components considered present a negligible thermal mass during the system start up. Contribution of the various components are similar (between 50-100 MWh/day) except that for the radiators (13 MWh). Results show that the entire system requires about 330 MWh of energy to reach the quasi steady state conditions after the night shutdown. This means that the energy absorbed is not negligible, especially if compared with the total amount required to the entire network in a day (about 10-15 GWh). Also considering that the extra exergy supplied to cover the peak is about 440 MWh, 330 MWh represents a large fraction of heat, highlighting the impact of the thermal masses. Results show that a different management of the network could provide significantly benefits. Among the options are a) thermal storage charged during the whole night to keep higher the water mass flow in a larger part of the network, b) the heat stored in the heating circuit and substation could be specifically exploited c) avoid night switching-off and prefer night attenuation.

7. Nomenclature

A: incidence matrix
c: specific heat, J/(kg K)
D: pipe diameter, m

E: energy, J
G: mass flow rate, kg/s
H: total entalpy, J/kg
k: thermal conductivity W/(mK)
K: stiffness matrix
L: pipe length, m
L: melting latent heat, J/kg
M: mass matrix, kg
P: pressure matrix, Pa
R: fluidynamic resistance, kg/(s Pa)
S: source term, W/m3
t: time, s
T: temperature, _C
v: velocity, m/s
Greek symbols
ρ : density, kg/m3
Φ : heat power W
Subscripts and superscripts
BC: boundary conditions
env: environmental
net: network
out: output p: pumping
SUP: supply
RAD: radiator
RADFLOOR: radiant floor
RET: return

8. References

[1] Wahlroos, M., Pärssinen, M., Manner, J., & Syri, S. (2017). Utilizing data center waste heat in district heating–Impacts on energy efficiency and prospects for low-temperature district heating networks. *Energy*, *140*, 1228-1238.

[2] Carotenuto, A., Figaj, R. D., & Vanoli, L. (2017). A novel solar-geothermal district heating, cooling and domestic hot water system: Dynamic simulation and energy-economic analysis. *Energy*, *141*, 2652-2669.

[3] Winterscheid, C., Dalenbäck, J. O., & Holler, S. (2017). Integration of solar thermal systems in existing district heating systems. *Energy*, *137*, 579-585.

[4] Bačeković, I., & Østergaard, P. A. (2018). A smart energy system approach vs a non-integrated renewable energy system approach to designing a future energy system in Zagreb. *Energy*, *155*, 824-837.

[5] Werner, S. (2017). International review of district heating and cooling. *Energy*, *137*, 617-631.

[6] Perpar, M., Rek, Z., Bajric, S., & Zun, I. (2012). Soil thermal conductivity prediction for district heating pre-insulated pipeline in operation. *Energy*, *44*(1), 197-210.

[7] Leśko, M., Bujalski, W., & Futyma, K. (2018). Operational optimization in district heating systems with the use of thermal energy storage. *Energy*, *165*, 902-915.

[8] Brand, M., Thorsen, J. E., & Svendsen, S. (2012). Numerical modelling and experimental measurements for a low-temperature district heating substation for instantaneous preparation of DHW with respect to service pipes. *Energy*, *41*(1), 392-400.

[9] Gadd, H., & Werner, S. (2013). Daily heat load variations in Swedish district heating systems. *Applied Energy*, *106*, 47-55.

[10] Vandermeulen A, van der Heijde B, Helsen L. Controlling district heating and cooling networks to unlock flexibility: A review. Energy
2018;151:103–15. doi:10.1016/j.energy.2018.03.034.

[11] Luthander, R., Widén, J., Munkhammar, J., & Lingfors, D. (2016). Self-consumption enhancement and peak shaving of residential photovoltaics using storage and curtailment. *Energy*, *112*, 221-231.

[12] Barzin, R., Chen, J. J., Young, B. R., & Farid, M. M. (2015). Peak load shifting with energy storage and price-based control system. *Energy*, *92*, 505-514.

[13] Romanchenko, D., Kensby, J., Odenberger, M., & Johnsson, F. (2018). Thermal energy storage in district heating: Centralised storage vs. storage in thermal inertia of buildings. *Energy conversion and management*, *162*, 26-38.

[14] Dominković, D. F., Gianniou, P., Münster, M., Heller, A., & Rode, C. (2018). Utilizing thermal building mass for storage in district heating systems: Combined building level simulations and system level optimization. *Energy*, *153*, 949-966.

[15] Guelpa, E., & Marincioni, L. (2019). Demand side management in district heating systems by innovative control. *Energy*, *188*, 116037.

[16] Vandermeulen, A., Reynders, G., van der Heijde, B., Vanhoudt, D., Salenbien, R., Saelens, D., & Helsen, L. (2018). Sources of energy flexibility in district heating networks: building thermal inertia versus thermal energy storage in the network pipes. In *Proceedings of the Urban Energy Simulation Conference 2018* (pp. 1-9). University of Strathclyde.

[17] Basciotti Daniele, Judex Florian, Pol Olivier, Schmidt Ralf-Roman. Sensible heat storage in district heating networks: a novel control strategy using the network as storage. In: Conference proceedings of the 6th international renewable energy storage conference IRES, Berlin, Germany; 2011.

[18] Mishra A. K., Jokisalo J., Kosonen R., Kinnunen T., Ekkerhaugen M., Ihasalo H., and Martin K. Demand response events in district heating: Results from field tests in a university building. Sustainable Cities and Society, 47, 101481, 2019.

[19] GKensby J., Tr¨uschel A., and Dalenb¨ack J. O. Potential of residential buildings as thermal energy storage in district heating systems–results from a pilot test. Applied Energy, 137, 773-781, 2015.

[20] Dominkovi´c D. F., Gianniou P., M¨unster M., Heller A., and Rode C. Utilizing thermal building mass for storage in district heating systems: Combined building level simulations and system level optimization. Energy, 153, 949-966, 2018.

[21] Gu, W., Wang, J., Lu, S., Luo, Z., & Wu, C. (2017). Optimal operation for integrated energy system considering thermal inertia of district heating network and buildings. *Applied Energy*, *199*, 234-246.

[22] Lund, H. (2018). Renewable heating strategies and their consequences for storage and grid infrastructures comparing a smart grid to a smart energy systems approach. *Energy*, *151*, 94-102.

[23] Hennessy, J., Li, H., Wallin, F., & Thorin, E. (2019). Flexibility in thermal grids: a review of short-term storage in district heating distribution networks. *Energy Procedia*, *158*, 2430-2434.

[24] Turski, M., Nogaj, K., & Sekret, R. (2019). The use of a PCM heat accumulator to improve the efficiency of the district heating substation. *Energy*, *187*, 115885.

[25] S. Stinner, K. Huchtemann, and D. Müller, "Quantifying the operational flexibility of building energy systems with thermal energy storages," Appl. Energy, vol. 181, pp. 140–154, Nov. 2016

[26] Frederiksen, S., & Werner, S. (2013). District heating and cooling. Studentlitteratur.

[27] https://ec.europa.eu/eurostat/documents/3217494/5634673/KS-43-02-042-EN.PDF/32e10ad4-43a3-4635-97f3-01b28ed6ba18

[28] Guelpa, E., & Verda, V. (2020). Automatic fouling detection in district heating substations: Methodology and tests. Applied Energy, 258, 114059.

[29] Sandersen C., Skov M., and Honore K. A manual for how to use existing buildings' heat profiles to improve the design and operation of buildings. Energy and Buildingstech. rep., HOFOR A/S, 2018.

[30]Guelpa, E. (2016). Modeling Strategies for Multiple Scenarios and Fast Simulations in Large Systems: Applications to Fire Safety and Energy Engineering: Thesis Submitted for the Degree of Doctor of Philosophy.

[31] U.S. Environmental Protection Agency. Drinking Water Requirements for States and Public Water Systems. Available online June 2020: https://www.epa.gov/dwreginfo/drinking-water-regulations

[32] Immergas, AUDAX TOP ErP and integrated systems Available online June 2020: https://www.immergas.com/imp/006J0/AUDAX-TOP-ErP-S226-GB.pdf

[33] Lund, H., Werner, S., Wiltshire, R., Svendsen, S., Thorsen, J. E., Hvelplund, F., & Mathiesen, B. V. (2014). 4th Generation District Heating (4GDH): Integrating smart thermal grids into future sustainable energy systems. Energy, 68, 1-11.

[34] Gao, L., Hwang, Y., & Cao, T. (2019). An overview of optimization technologies applied in combined cooling, heating and power systems. Renewable and Sustainable Energy Reviews, 114, 109344.

[35] Calise, F., di Vastogirardi, G. D. N., d'Accadia, M. D., & Vicidomini, M. (2018). Simulation of polygeneration systems. Energy, 163, 290-337.

[36] Soutullo, S., Bujedo, L. A., Samaniego, J., Borge, D., Ferrer, J. A., Carazo, R., & Heras, M. R. (2016). Energy performance assessment of a polygeneration plant in different weather conditions through simulation tools. Energy and Buildings, 124, 7-18.